Geomorphology 418 (2022) 108477

Contents lists available at ScienceDirect

Geomorphology

journal homepage: www.journals.elsevier.com/geomorphology

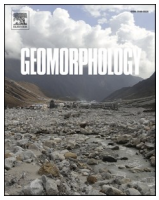

Limits to coseismic landslides triggered by Cascadia Subduction Zone earthquakes

Alex R.R. Grant [a,*], William T. Struble [b], Sean R. LaHusen [c]

[a] U.S. Geological Survey, Earthquake Science Center, Seattle, WA, USA
[b] Department of Geosciences, University of Arizona, Tucson, AZ, USA
[c] U.S. Geological Survey, Geology Minerals Energy and Geophysics Science Center, Moffett Field, CA, USA

ARTICLE INFO

Keywords:
Landslides
Coseismic
Cascadia Subduction Zone
Oregon Coast Range

ABSTRACT

Landslides are a significant hazard and dominant feature throughout the landscape of the Pacific Northwest. However, the hazard and risk posed by coseismic landslides triggered by great Cascadia Subduction Zone (CSZ) earthquakes is highly uncertain due to a lack of local and global data. Despite a wealth of other geologic evidence for past earthquakes on the Cascadia Subduction Zone, no landslides have been definitively linked to such earthquakes, even in areas otherwise highly susceptible to failure. While shallow landslides may not leave a lasting topographical signature in the landscape, there are thousands of deep-seated landslides in Cascadia, and these deposits often persist for hundreds of years and multiple earthquake cycles. Synthesizing newly developed inventories of dated large deep-seated landslides in the Oregon Coast Range, we use statistical methods to estimate the proportion of these types of landslides that could have been triggered during past great Cascadia Subduction Zone earthquakes. Statistical analysis of high-precision dendrochronology ages of landslide-dammed lakes and surface roughness-dated bedrock landslides reveal Cascadia Subduction Zone earthquakes may have triggered 0–15 % of large deep-seated landslides in the Oregon Coast Range over multiple earthquake cycles. Our results refine estimates from previous studies and further suggest that coseismic triggering accounts for a small fraction of the total deep-seated bedrock landslides mapped in coastal Cascadia. However, if the real rate of coseismic landslide triggering during CSZ earthquakes is near our estimated upper bound for the 1700 CSZ earthquake, we estimate up to 2400 coseismic large deep-seated landslides could occur in the Oregon Coast Range in a single earthquake. These findings suggest Cascadia is consistent with global observations from other subduction zones and that coseismic landslides may still represent a serious geohazard in the region.

1. Introduction

Earthquake-triggered landslides are a major coseismic hazard that can result in considerable loss of life and impacts to the built environment (e.g., Petley, 2012). The impacts of earthquake-triggered (coseismic) landslides range from immediate (e.g., damage to infrastructure), cascading (landslide dam formation and subsequent outburst flooding), and long term (landscape evolution; Fan et al., 2019 and references therein). While landslides triggered by shallow crustal faults have been studied extensively (e.g., Bommer and Rodríguez, 2002; Keefer, 1984; Marc et al., 2016; Meunier et al., 2007; Valagussa et al., 2019), uncertainty in the expected distribution, magnitude, type, and impacts of coseismic landslides during great (Magnitude [M] $\geq$ 8.0) megathrust earthquakes is much higher given the relative paucity of studies on landslides triggered (or lack thereof) by great earthquakes, with well documented inventories only existing for three events (Lacroix et al., 2013; Serey et al., 2019; Wartman et al., 2013). This uncertainty is particularly acute in the Pacific Northwest of the United States, where onshore evidence of the impacts of the last great earthquake, a M8.7–9.2 on January 26, 1700 (e.g., Nelson et al., 1995; Satake et al., 2003; Atwater et al., 2005), is limited to surviving oral histories, tsunami sands, and limited ground failure evidence scattered along the coastal regions of Cascadia.

Inland impacts of pre-1700 CSZ earthquakes are even more limited to observations of lacustrine turbidites (e.g., Karlin et al., 2004; Leithold et al., 2018) and older paleoliquefaction features possibly associated with these events (Rasanen et al., 2021). While previous efforts have used paleoliquefaction evidence (Obermeier, 1995) and fragile geologic

* Corresponding author.
E-mail address: agrant@usgs.gov (A.R.R. Grant).

https://doi.org/10.1016/j.geomorph.2022.108477
Received 21 April 2022; Received in revised form 27 September 2022; Accepted 28 September 2022
Available online 3 October 2022

features (McPhillips and Scharer, 2021) to estimate CSZ paleoshaking intensities, the number of landslides triggered by great CSZ earthquakes, and therefore magnitude of coseismic landslide hazard, remains unknown from existing studies. Scant global records of detailed megathrust earthquake triggered landslide inventories (N = 3, Lacroix et al., 2013; Serey et al., 2019; Wartman et al., 2013), and estimates from the 1964 Alaska earthquake (> 10,000 landslides, Keefer and Wilson, 1989), suggest fewer coseismic landslides may be triggered in great subduction zone earthquakes than during large magnitude crustal earthquakes (Tanyaş et al., 2017). However, this small pool of global data limits our ability to confidently predict future CSZ earthquake triggered landslide impacts. First nation oral histories attributable to the 1700 earthquake describe a highly destructive landslide in southern Vancouver Island, Canada (Ludwin et al., 2005), but no other direct landslide evidence has been found for the 1700 earthquake (LaHusen et al., 2020; Struble et al., 2020), and the exact location of this slide is unknown. Several candidate 1700 landslides in Oregon and Washington, United States of America (USA) have been identified (Anderson, 2009; Bush, 2020; Leithold et al., 2018; Schulz et al., 2012) but lack precise CSZ earthquake coeval ages that could be used to infer coseismic triggering. Three large rockslides on the coast of Oregon remain some of the best evidence of CSZ triggered landslides, as the site-specific modeling study of Schulz et al. (2012) found existing slide geometries impossible to generate without strong shaking. One of the challenges in finding landslide evidence from past CSZ earthquakes is only a fraction of all coseismic landslides are likely to be large deep-seated landslides that could be preserved in the landscape for hundreds of years. While great earthquakes may trigger larger slides on average than smaller magnitude events (Jibson and Tanyaş, 2020), small, shallow soil slides that are less unlikely to be well preserved in the landscape are still expected to be the dominant mode of coseismic landsliding during a CSZ earthquake. However, as in previous studies in the region, this work focuses on less common large deep-seated slides due to the preservation of these features in the landscape to draw inferences about the impacts of past CSZ earthquakes.

Though little is known about the onshore effects of Cascadia earthquakes, recent landslide mapping and dating work is beginning to shed light on the tens of thousands of landslides that are ubiquitous throughout the Oregon Coast Range, USA (OCR). While shallow landslides and debris flows are common during the rainy season (Montgomery, 2001; Penserini et al., 2017; Schmidt et al., 2001; Stock and Dietrich, 2003), few deep-seated landslides have been observed in the past 100 years, which previously led to speculation that these bedrock slides are primarily a result of CSZ earthquakes (e.g., Roering et al., 2005; Schulz et al., 2012). While recent work (e.g., LaHusen et al., 2020) has suggested a strong hydrologic presence in landslide triggering, it's unclear how many CSZ earthquake triggered landslides could be preserved in the OCR. Deep-seated bedrock landslides in the OCR exhibit a conspicuous topographic form, where benchy, low-relief surfaces demarcate relict slope failures with landscape residence times >100 kyr (Almond et al., 2007; Roering et al., 2005). To date, over 20,000 deep-seated landslides have been mapped throughout the OCR (Franczyk et al., 2019; LaHusen et al., 2020). Of these tens of thousands of landslides deposits, hundreds have formed dams that persist today. These dams often form ephemeral or long-lived lakes upstream, which drown and kill trees that were previously occupying the valley floor. Dendrochronology can then be used to precisely date the timing of tree death, sometimes with sub-annual accuracy, and therefore the timing of slope failure (e.g., Pringle, 2014; Šilhán, 2020). Thus, landslide-dammed lakes represent a means of confidently modeling the timing of dam formation, and possibly revealing coseismic triggering when the timing of past-earthquakes is known, in a way that radiocarbon dating is incapable of due to the high relative uncertainty (e.g., Struble et al., 2020). Importantly, 22 individual landslide dams in the OCR have now been dated using dendrochronology, yet no landslide dams match the 1700 C.E. date of the last CSZ earthquake (Struble et al., 2021).

Here, we use statistical methods to compute the implied triggering rate of large, deep-seated landslides by great CSZ earthquakes from two dated landslide inventories in the Oregon Coast Range. We first leverage the aforementioned landslide dam ages in the OCR (Struble et al., 2020, 2021), which include dendrochronology-derived dates, to estimate the proportion of landslide dams that may have formed during the 1700 CSZ earthquake as well as during multiple earthquakes over the past 1000 years. Second, we compare an inventory of nearly 10,000 deep-seated bedrock landslide ages in the central OCR (LaHusen et al., 2020) to synthetic landslide inventories composed of different proportions of coseismic slides to place constraints on possible CSZ triggering rates of large bedrock landslides. These two sets of results are then combined to place upper bounds on the overall rate of large deep-seated landslide triggering during great Cascadia Subduction Zone earthquakes in the Oregon Coast Range.

2. Methods and data

To estimate the fraction of large-deep seated landslides in the OCR triggered by great CSZ earthquakes, we developed a three-part analysis to model (Section 2.1) limits on the number of coseismic landslide dams triggered by the last CSZ earthquake in 1700 C.E., (2.2) the percent of landslide dams triggered by CSZ earthquakes over multiple earthquake cycles during the last 1000 years, and (2.3) the proportion of bedrock landslides (including primarily non-dam forming landslides) triggered by CSZ-earthquakes, using an independent dataset of nearly 10,000 landslides in the OCR dated using topographic surface roughness. An important assumption in this work is that coeval earthquake and landslide ages imply seismically-trigged slope failure. Overlapping ages of landslide dams and past CSZ earthquakes could also be caused by coincidental triggering from other sources, and we address this lack of causal information in Section 2.2 of our methods. To estimate a range of large deep-seated landslides triggered by great CSZ earthquakes in the OCR, we utilized high-precision age constraints from 21 landslide dams from the work of Struble et al. (2020, 2021) and approximated calibrated surface roughness age estimates of 9938 large bedrock landslides in the Tyee Formation of LaHusen et al. (2020), shown in Fig. 1. Also shown in Fig. 1 are the expected peak ground accelerations from a suite of full margin M9.0 CSZ earthquake simulations (Wirth et al., 2021). Peak ground accelerations range from approximately 0.2–0.6 g across the OCR, which is sufficient to trigger widespread landsliding where steep slopes are present, and lines up with a peak in observed coseismic landslides found in the global record (Tanyaş et al., 2017). Though the Struble et al. (2021) database includes additional landslide dams east of our study area, we omitted sites where expected shaking is <0.2 g to focus this study on landslide dams most likely to be triggered by past CSZ earthquake shaking.

In an effort to locate and date landslides that may have been triggered by the 1700 CSZ earthquake, Struble et al. (2021) identified 226 landslide dams in the OCR (Fig. 1) from 0.91 m (3 ft) resolution lidar digital elevation models (OLC and DOGAMI, 2022). These landslide dams include landslide-dammed lakes, previous lakes now filled with sediment, and partial valley-filling landslides, collectively defined as 'landslide dams.' To establish age constraints on the mapped landslides, Struble et al. (2020, 2021) utilized dendrochronology of ghost forests submerged by landslide-dammed lakes. Interannual variability in tree ring growth often permits dating landslide dams with subannual accuracy, which allows for establishing linkages between dam formation and known triggering events. Through correlation of ring measurements extracted from drowned Douglas-fir trees with existing western Oregon tree ring chronologies, Struble et al. (2020, 2021) dated 22 landslide-dammed lakes in the OCR, finding that 18 well-dated slides post-date the 1700 CSZ earthquake. While they observed temporal clustering of landslides, most notably in the winter of 1889/90, likely corresponding to major regional flooding in February 1890, no landslide was clearly linked with the 1700 CSZ earthquake. Three landslide-dammed lakes have maximum ages (the lack of preserved bark at these sites precluded

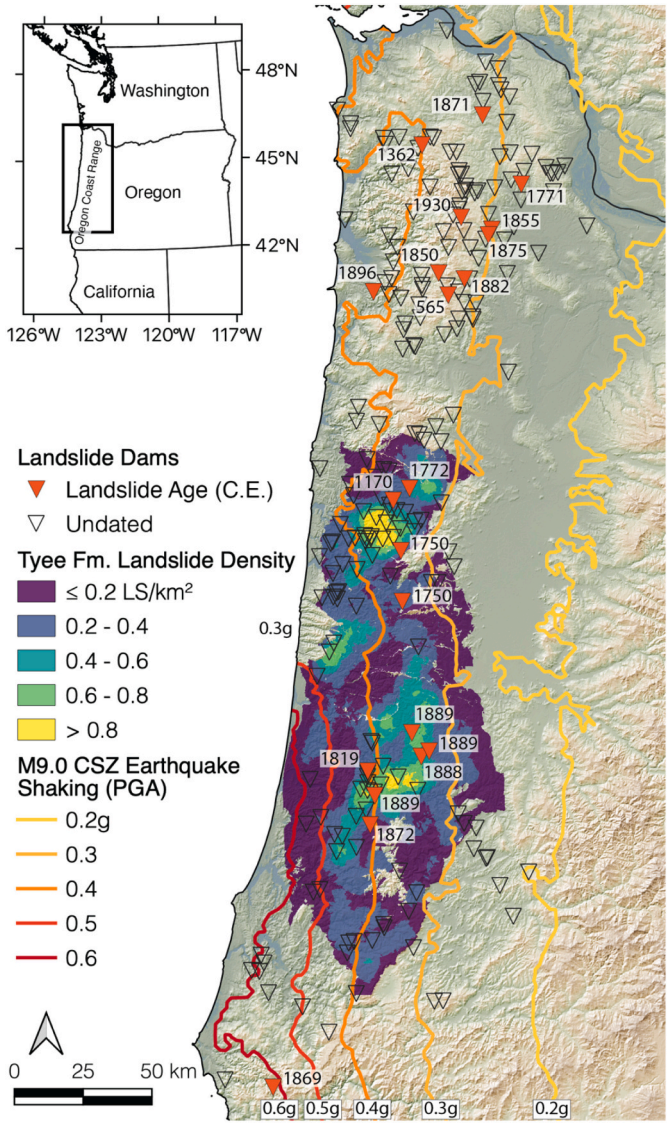

Fig. 1. Landslides and shaking estimates of the Oregon Coast Range. Landslide dams and ages from subannual dendrochronology (or maximum ^{14}C dates where more precise ages are unavailable) from Struble et al. (2021) shown as labeled red triangles. Areal density of large bedrock landslides mapped by LaHusen et al. (2020) shown as filled contours. Expected (median) peak ground accelerations (PGA) for a M9.0 CSZ earthquake (Wirth et al., 2021) shown in colored contours.

subannually accurate dating) that pre-date the 1700 CSZ earthquake, and two of these landslide dates fall within measurement uncertainty of pre-1700 CSZ earthquakes: Buttermilk Lake (1170–1260 C.E.) potentially corresponds with the third most recent 'T3' (868 ± 58ybp) event and Spruce Run Lake (1362–1402 C.E.) with the penultimate 'T2' earthquake (552 ± 83 ybp; Goldfinger et al., 2012; Struble et al., 2021). At this time, however, dating uncertainties for both CSZ earthquakes and landslides preclude a clear linkage between the two.

2.1. Part 1: limits to the 1700 CSZ earthquake landslide dam triggering rate

To estimate the number of landslide dams that may have been triggered by the 1700 CSZ earthquake, we first assumed that the 226 landslide dams presented by Struble et al. (2021) reflect the total population of landslide dams in the OCR. Second, we considered only the landslide dam ages of Struble et al. (2020, 2021) that are from 1700 or younger (N = 18). Landslide dams with known ages before 1700 (N = 3) were omitted, as they had already mobilized sufficiently to form a landslide dam prior to the 1700 earthquake, and any reactivation or additional movement is not part of the landslide dam triggering and formation rate we aimed to capture in this analysis. Xu et al. (2021), in an InSAR analysis of ALOS and ALOS-2 data from 2007 to 2019, found very few landslides within our study region of the OCR have detectable movements despite the widespread mapped landslides in the region. While displacement rates of landslides included in this study could have changed over time, we assume the lack of present-day movement of these slides supports the assumption that the date of tree-downing from lakes closely reflects the triggering event (earthquake or aseismic), and not a delayed response due to creeping landslides.

Given these assumptions, we set up a Monte-Carlo sampling simulation to estimate possible rates of coseismic landslide dam triggering given 0 observations of 1700-aged landslides in 18 samples from a total population of 226 landslide dams. Specifically, for modeled rates of landslide dam triggering of 0–50 % (0–113 dams in increments of one landslide dam), we drew 18 samples from the total population of 226 that includes our modeled amount of 'CSZ 1700 earthquake' landslide dams, and recorded if any of the 18 samples contain a 'coseismic' landslide dam. For each modeled rate of landslide dam triggering, we repeated this process 250 times (N_{total}), recording the number of samples (N_{null}) with no observations of coseismic landslide dams. We then computed the likelihood of observing no coseismic landslide dams for that modeled rate of landslide dam triggering as:

$$P_{N=0} = \frac{N_{total} - N_{null}}{N_{total}} \quad (1)$$

To estimate the uncertainty of these predictions, we repeatedly draw rounds of 250 samples until we have a total of 10,000 iterations for each modeled landslide rate to compute a mean, and standard deviation, of the probability of observing zero 1700 coeval landslide dams.

2.2. Part 2: percent of landslide dams triggered over multiple CSZ earthquake cycles

In the last 1000 years, onshore and offshore evidence strongly suggest the occurrence of 2–3 great CSZ earthquakes (e.g., Atwater and Hemphill-Haley, 1997; Kelsey et al., 2002; Witter et al., 2003; Nelson et al., 2006; Goldfinger et al., 2017; Nelson et al., 2021). To further leverage the available Struble et al. (2020, 2021) landslide dam datasets and place constraints on the proportion of coseismic OCR landslide dams triggered over multiple CSZ earthquakes, we repeated the analysis from Part 1 (2.1) with two important modifications. First, we used 21 dendrochronology ages of landslide dams from Struble et al. (2020, 2021), which include those that predate the 1700 CSZ earthquake. While the complete Struble et al. (2020, 2021) databases include 22 ages of landslide dams, Sunago Lake was omitted from this analysis due to poor age constraint (four possible ranges covering nearly 200 years). Second, given the uncertainty in the timing of pre-1700 CSZ earthquakes, definitive linkages cannot be made between the older landslide dams of Struble et al. and existing CSZ earthquake chronologies (e.g., Goldfinger et al., 2012; Nelson et al., 2021). Therefore we computed likelihoods that zero, one, or two CSZ-triggered landslide dams are observed in a sample of 21 from the total population of 226 dams. This allowed us to account for the possibility that neither, one, or two of the older landslide dams were triggered by a pre-1700 CSZ earthquake. As in Part 1 (2.1), simulations with 0–113 modeled CSZ triggered landslide dams were repeated for 10,000 iterations to estimate the likelihood of matching the observed data of Struble et al. (2020, 2021).

2.3. Part 3: percent of bedrock landslides triggered over multiple CSZ earthquake cycles

LaHusen et al. (2020) mapped 9938 deep-seated bedrock landslides

in the Tyee and Elkton Formations of the central OCR, shown as density contours in Fig. 1. Landslides were mapped from 0.91 m resolution (3 ft) bare-earth lidar topography over an area of 15,000 km^2. Only coherent rotational and translational slides larger than 5000 m^2 with a minimum dimension of at least 100 m were included in the LaHusen et al. (2020) dataset. These large bedrock landslides are consistent with failures that may occur during great CSZ earthquakes (e.g., Jibson and Tanyaş, 2020) and with the scale of landslides considered in the Struble et al. (2020, 2021) landslide dam studies. LaHusen et al. (2020), expanding on earlier work linking landslide deposit surface roughness to age (Booth et al., 2017; LaHusen et al., 2016), used 14 independent age constraints from ^{14}C and dendrochronology of bedrock landslides to calibrate an age-roughness curve for the central OCR. This calibrated age-roughness curve represents how initially rough landslide deposits smooth over time and was applied to their full bedrock landslide inventory to examine spatio-temporal trends in landslide occurrence. LaHusen et al. (2020) found no significant increase in landslide occurrence near the times of past large CSZ earthquakes, concluding that more than half the landslides in their study were triggered by rainfall or other non-CSZ sources.

While the deep-seated landslide inventory of LaHusen et al. (2020) lacks the dating precision and closed population of the first two phases of this study, its large size and position in the central OCR are used to place an independent constraint on coseismic landslide triggering during large CSZ earthquakes. Moreover, this dataset is not confined to landslide dams, but includes all deep-seated rotational and translational landslide deposits. LaHusen et al. (2020) developed a method to estimate the relative contributions from uniform 'background' landslide triggering and pulses of coseismic landslides by generating synthetic landslide inventories. However, LaHusen et al. (2020) only considered coseismic rates of landslide triggering of 0, 50, and 100 %. Here we reanalyze the LaHusen et al. (2020) landslide chronology using an updated methodology to assess the goodness of fit between coseismic triggering rates from 0 to 50 % and the observed data, allowing for a more thorough assessment of bedrock landslides in the OCR.

Following LaHusen et al. (2020), we generated synthetic landslide inventories and compared them to the observed age-roughness distribution of bedrock landslides in the central OCR. The purpose of this analysis is to account for uncertainty in the roughness-dating technique to estimate the range of coseismic landslide triggering rates that are consistent with the data. Unlike the precise nature of dendrochronology, landslides of the same age may have different roughness values, which introduces error when using roughness as a proxy for age. Synthetic landslide inventories allow us to account for this error by incorporating variance in roughness values for landslides of the same age, like those that may occur simultaneously during a large CSZ earthquake. Synthetic landslide inventories were generated in a 6-step process, described in more detail below as: (1) Calibrate an age-roughness regression with available landslide ages that predicts how landslide roughness decreases over time, (2) compute and remove preservation bias effects from the observed inventory, (3) generate uniform counts of 'background' landslides ages (landslides not triggered by earthquakes) as samples from random-normal roughness distributions for each model timestep, (4) generate pulses of coseismic landslides as samples from random-normal roughness distributions at dates of known earthquakes, (5) combine the products of steps 3 and 4 and impose the preservation bias computed in step 2, (6) repeat 3–5 for all modeled coseismic landslide triggering rates.

From LaHusen et al. (2020), bedrock landslide age in the central OCR can be expressed as:

$$age = 1.428*10^{-4}e^{-0.1762r} \quad (2)$$

where r is landslide deposit roughness as measured by a 20 m scale two-dimensional continuous wavelet transform from a lidar digital elevation model, and *age* is in years before 2019 (to avoid negative ages being assigned to post-1950 historical landslides). Assuming constant rates of background landslide triggering through time, changes in the observed long-term rates of landslide age-frequency were interpreted as a preservation bias by LaHusen et al. (2020). This preservation bias, refit as a best-fit 2nd order polynomial to the observed landslide age-frequency distribution was described as:

$$R(t) = 4.03 - 0.004t + 2.0*10^{-6}t^2 \quad (3)$$

where t is time in years and R is the annual rate of landslide triggering. This trend in the age-frequency curve (preservation bias) was then normalized to the most-recent time period and removed from the observed landslide counts to estimate the expected total number of deep-seated landslides in the central OCR in the last 1000 years. For each modeled rate of CSZ coseismic landslide triggering (0–50 % in 0.25 % increments), the total number of landslides in the past 1000 years is partitioned into background and coseismic counts, uniformly distributed across modeled earthquake dates and 50-year time steps respectively. For each time step, or earthquake date, modeled landslides are sampled from a random-normal distribution of roughness given by rearranging Eq. (2) for a specific age and standard deviation of roughness ($8.4 * 10^{-4}m^{-1}$) from LaHusen et al. (2020). LaHusen et al. (2020) computed the standard deviation of roughness from a set of similarly-aged landslides in the OCR (with estimated ages near 1700 C.E.). Landslide ages were then calculated via Eq. (2) for the combined background and coseismic synthetic inventories to compute a modeled age-frequency distribution of landslides. For each modeled rate of CSZ coseismic landslide triggering, 1000 iterations of synthetic landslide inventories were generated to compute a mean age-frequency distribution.

3. Results

The results of Part 1 (2.1), where we estimate the range of landslide dams trigged by the CSZ 1700 earthquake, are shown in Fig. 2. For each number of modeled CSZ-triggered landslide dams, Fig. 2 shows the likelihood of observing zero coseismic landslides, given a dataset of 18 known ages from 226 total landslide dams. Highlighted values in Fig. 2 mark the 50, 25, 10, and 5 % likelihood levels of matching the observed record, and reflect the median, and various thresholds that could be adopted as likely (25 %), possible upper limit (10 %), and an even higher upper bound (5 %). These values imply that, of the 226 observed dams in the OCR, 8, 16, and 26 dams could have been triggered by the 1700 CSZ earthquake for the 50 %, 25 %, and 10 % likelihood cases, respectively. Higher counts of modeled coseismic landslide dams (i.e., 25–50 % of all landslide dams) are not shown in Fig. 2 as the computed likelihoods are ~0 %. Given zero of the 18 considered landslide dam ages match the 1700 earthquake from a total of 226 landslide dams, we estimate the possible upper limit to total fraction of landslide dams caused by the 1700 earthquake is ~12 % (26 landslide dams).

In Part 2 of our analysis (2.2), we define the likely range of coseismic landslide dam triggering as the 10th – 90th percentiles of simulation results that match the dendrochronology landslide dam ages of Struble et al. (2020, 2021). This range was selected as a conservative estimate of possible 'true' rate of coseismic landslide triggering as it captures the central 80 % of the simulations that match the available dendrochronology data while still reflecting differences between different scenarios. We also defined the upper limit of expected coseismic landslide dam triggering to be the 90th percentile of a given scenario. Additionally, we defined the most-likely rates of coseismic landslide dam triggering as a range from the 25th – 75th percentiles of the simulation results that match the observed record.

Fig. 3 shows the results of Part 2 of our analysis (2.2) of the longer multi-earthquake chronology of Struble et al. (2020, 2021), where 0–2 dated landslide dams may have been triggered by CSZ earthquakes prior to 1700. Fig. 3 shows the 10th – 90th percentiles (possible range of true

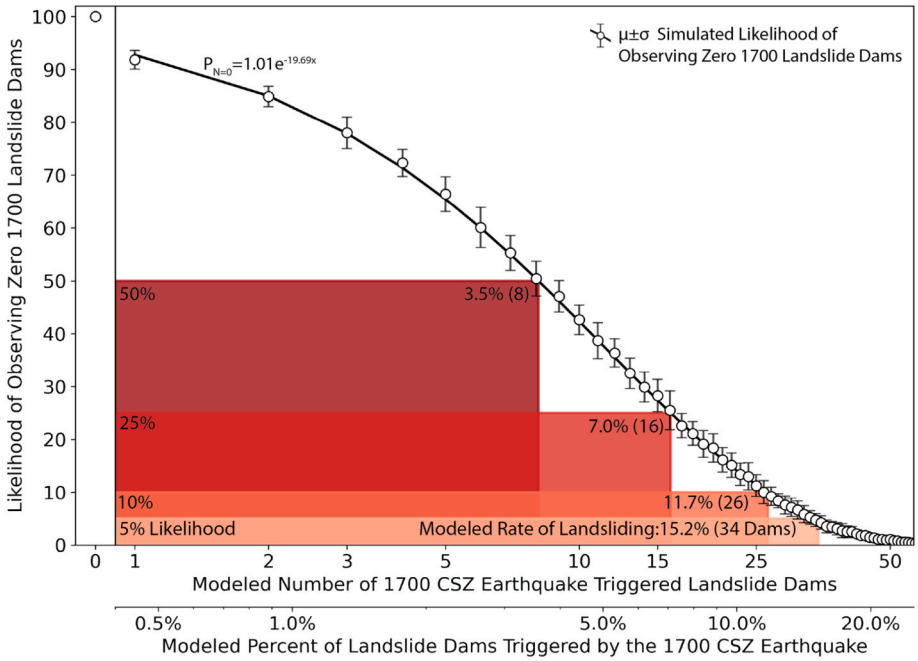

Fig. 2. Predicted likelihood (μ, plus or minus one standard deviation [σ]) of observing zero landslide dams triggered by the 1700 CSZ earthquake for modeled coseismic landslide dam triggering rates of 0–25 % (0–57 landslides, open circles). Filled boxes show corresponding rates of earthquake-triggered landslide dam formation during the 1700 CSZ earthquake for 50, 25, 10, and 5 % likelihood given zero 'true' observations in 18 samples of 226 total landslide dams (Struble et al., 2020, 2021).

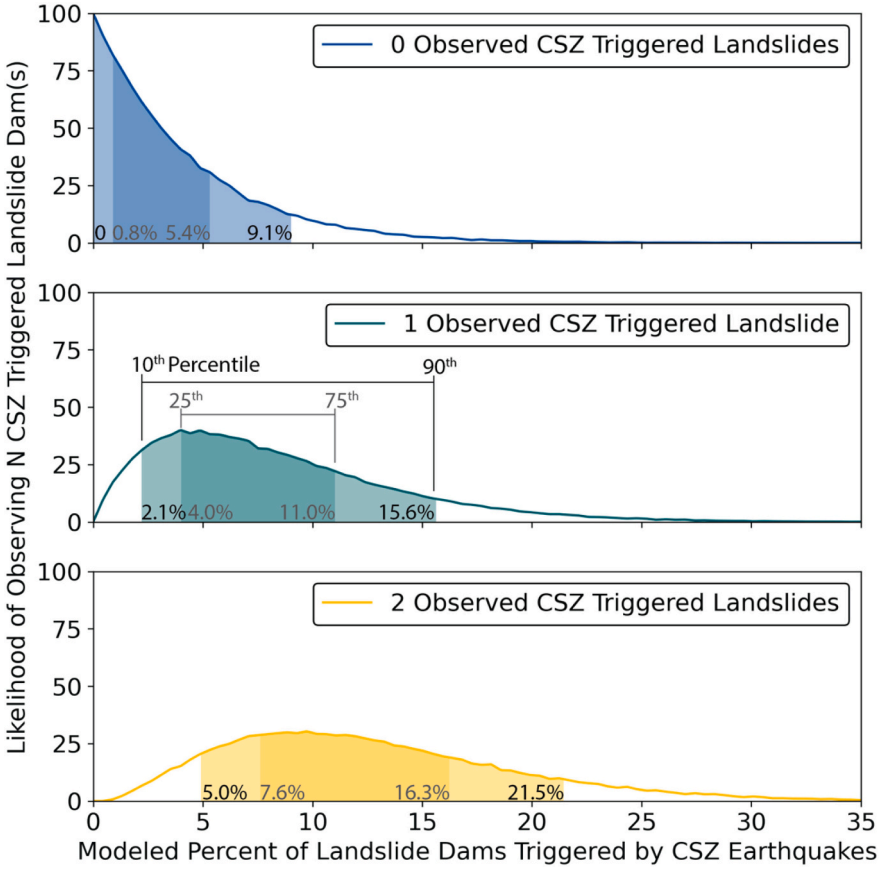

Fig. 3. Expected likelihoods of observing zero, one, or two CSZ earthquake-triggered landslide dams from 21 samples of 226 total landslide dams (Struble et al., 2020, 2021). Light shaded regions show the 10 – 90th percentiles of simulations matching the Struble et al. datasets assuming 0–2 true CSZ coseismic observations and corresponding total percent of coseismic landslide dams. Darker shaded regions show the same information for the 25 – 75th percentiles.

landslide triggering) and 25th – 75th percentile (most likely range) of simulations that match the null result of Struble et al. (2020, 2021) and ranges of CSZ earthquake dates (c.f. Walton et al., 2021). Given the available CSZ earthquake and landslide dam age data, this analysis covers the past 1000 years in the OCR, spanning 2–3 great CSZ earthquakes (Goldfinger et al., 2012; Nelson et al., 2021). Assuming both

overlaps in ages between CSZ earthquakes and landslide dams are evidence for true coseismic-triggering relationships, our predicted overall fraction of coseismic landslide dams rises to 5–22 %. Simulations where neither, or just one, of these landslide dams were triggered by CSZ earthquakes yield possible ranges of 0–9 %, or 2–15 %, respectively, of all OCR landslide dams may be earthquake-triggered. Combining, the average of these three scenarios gives a possible range of 2–15 % of all landslide dams in the OCR were triggered by CSZ earthquakes.

Results for Part 3 of this study (2.3), where synthetic landslide inventories were generated to measure goodness of fit to the observed record of LaHusen et al. (2020) are shown in Fig. 4 for coseismic triggering rates of 0, 5, 10, 25, and 50 %. Coseismic triggering rates from 0 to 50 % in 0.25 % increments were run but only a small subset of these results are shown to illustrate the results in Fig. 4. We calculated the fit of each synthetic scenario to the observed age-frequency landslide data of LaHusen et al. (2020) as root-mean-square-error (*rmse*), and coefficient of determination (r^2). Synthetic results match observed landslide age-frequency most closely for modeled coseismic triggering rates of 0–9.5 % ($r^2 > 0.95$, rmse remains near minimum, inset Fig. 4). The fit to observed data remains very good ($r^2 > 0.9$) for coseismic triggering rates up to 12 %. We repeated this analysis for the Nelson et al. (2021) Cascadia earthquake chronology, where two ruptures (1700 and ~1160) are modeled in the last 1000 years. In this scenario, the observed distribution of landslides is well explained ($r^2 > 0.9$) by coseismic landslide triggering rates of 0–12 %. Coseismic triggering rates consistent with this threshold of $r^2 > 0.9$ across both CSZ earthquake chronologies were adopted as a preferred solution to the available data (0–12 % coseismic landslide triggering).

4. Discussion

Through repeated simulation of the observed dendrochronology record of landslide dams in the Oregon Coast Range, we estimate the possible range of OCR landslide dams triggered by the 1700 CSZ earthquake is 0–12 % (0–26), shown in Fig. 2. While uncertainty in the exact dates of pre-1700 CSZ earthquakes prevent definitive linkages between the timing of landslide dam triggering and CSZ earthquakes, we estimate a possible overall percent of coseismic landslide dams in the OCR of 0–22 % (Fig. 3) given the 0–2 existing observations of CSZ earthquake-triggered landslide dams in the past 1000 years (Struble et al., 2020, 2021). Limits on coseismic landslide triggering from the landslide-dammed lake dendrochronology record agree with patterns of large bedrock landslides in the Tyee and Elkton Formations of the central OCR mapped and dated by LaHusen et al. (2020), where the observed time-frequency distribution of landslides is best modeled by synthetic landslide inventories composed of 0–12 % CSZ earthquake-triggered landslides (Fig. 4). Taken together, we estimate the total fraction of large CSZ earthquake-triggered landslides in the OCR to be 0–15 %, with lower ranges possible for individual (e.g., the 1700) earthquakes. While it is still possible no landslide dams or large bedrock landslides in the OCR have been triggered by great CSZ earthquakes, our results show that tens of landslide dams, and over a thousand large landslides triggered during CSZ earthquakes may exist and would still be consistent with the observations of LaHusen et al. (2020) and Struble et al. (2020, 2021).

To model how future high-precision (e.g., dendrochronology) landslide ages could affect our interpretations of CSZ landslide dam triggering rates, we repeated our analyses for hypothetical datasets of 25 to 50 total dated landslide dams. In this imagined expanded dataset of landslide dam ages, we allow for up to five matches to CSZ earthquake ages, assuming for the purposes of this exercise that coeval dates imply coseismic landslide dam triggering. For each new landslide dam chronology dataset, we compute the probability of matching 0–5 observations of CSZ coeval landslide dam ages following the same methodology as in Section 2.2. Plotted in Fig. 5 are the results of this suite of simulations, where each line is the distribution of likelihoods of matching 0–5 CSZ coeval samples given 25–50 known landslide dam ages. In all scenarios, increasing the number of well-constrained ages decreases the uncertainty of our estimates of coseismic triggering of landslide dams. In the extreme case, if we assume that the two existing ages overlapping with pre-1700 CSZ earthquakes are coseismic and that the next three landslide dam ages correspond with CSZ earthquakes (five matches in 25 ages), then our upper estimate on the overall percent of landslide dams triggered by CSZ earthquakes would rise to just under a third (32 %).

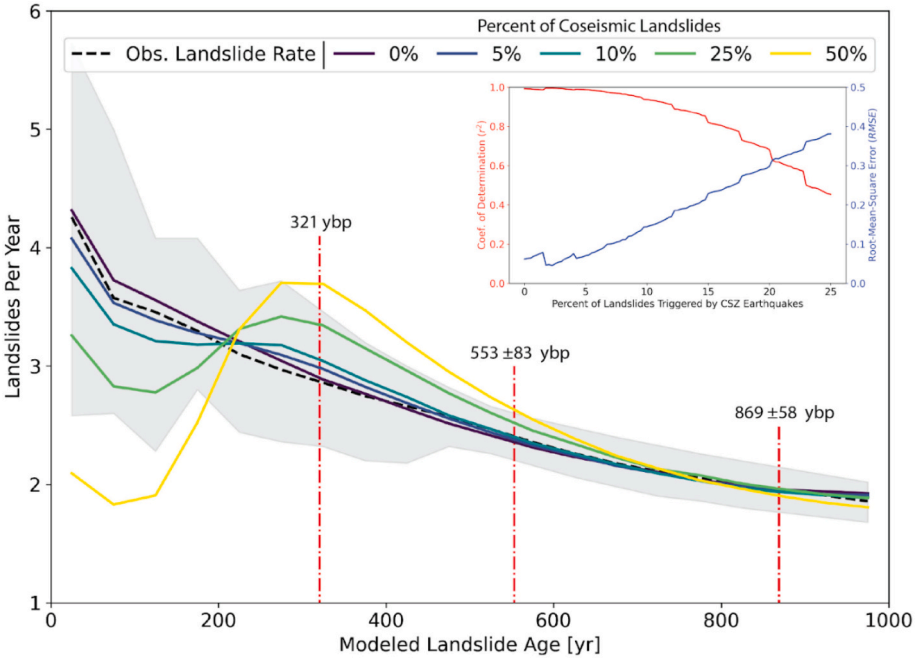

Fig. 4. Observed landslide rates for the past 1000 years (dashed black line, 1σ uncertainty in gray) and synthetic landslide inventories for total coseismic landslide triggering rates of 0–50 %. Synthetic inventories were constructed from background rates computed from the observed record and pulses of landslide triggering at inferred dates of full-margin CSZ earthquakes (Goldfinger et al., 2012, marked by red lines).

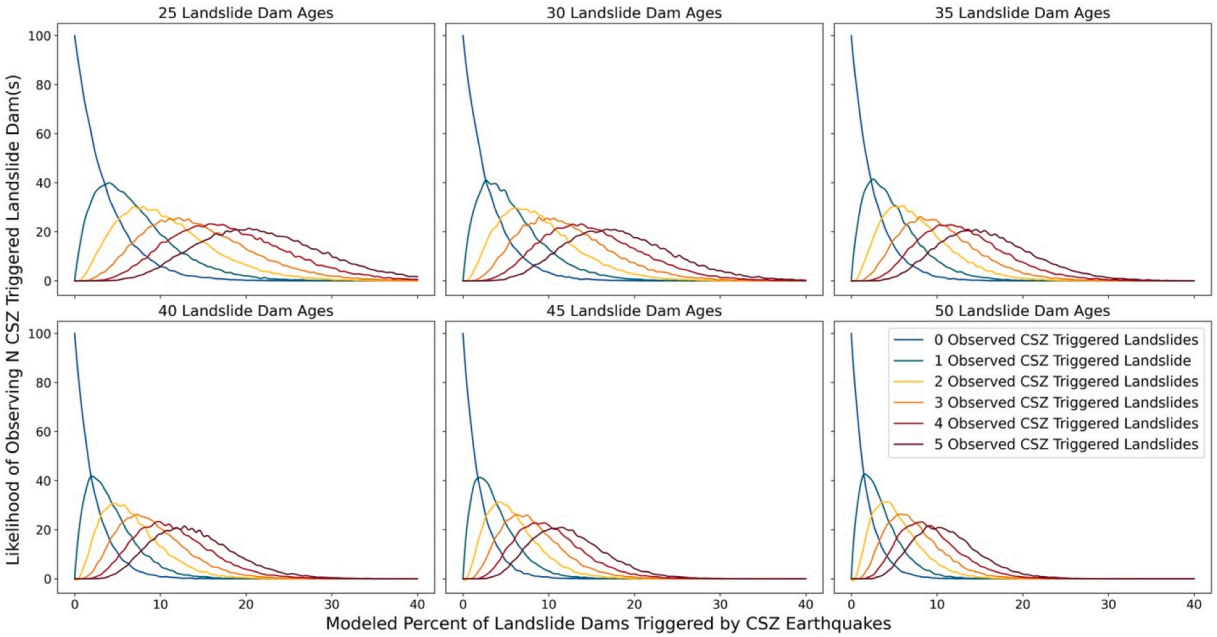

Fig. 5. Likelihood of observing exactly 0, 1, 2, 3, 4, or 5 coseismic landslide dams given models where 0–40 % of all landslide dams were triggered by CSZ earthquakes for 25–50 high-precision landslide dam ages.

Given the paucity of observations to date, a likely upper bound on the total percent coseismic landslide dams may be approximately 6–18 % in the case of finding 0–3 CSZ triggered landslide dams in the next ten high-precision ages. While these results don't exclude the possibility that many existing landslide dams were triggered during the last great CSZ earthquake, the effect of finding some coeval dates in the landslide-dammed lake record would not cause major shifts in implied rates of coseismic triggering. However, additional work to date landslides in the OCR and elsewhere in the CSZ would still have significant impacts. First, future landslide dam ages associated with the 1700 or older earthquakes would have the fundamental impact of removing the possibility that zero of these landslides are coseismic. Second, CSZ earthquake coeval dates will allow modeling of the shaking intensities at these sites to constrain past shaking estimates. Third, all new ages of OCR landslide dams (CSZ coeval or not) reduce the uncertainty in past coseismic landslide triggering rates and better constrain estimates of future impacts of CSZ earthquakes.

In part 3 of the analysis (2.3), we did not consider uncertainty in the date of pre-1700 earthquake occurrence. This simplification should not significantly affect our results, as the variance of landslide roughness for a specific age used in the modeling is much larger than the reported variance in age estimates for CSZ earthquakes, especially for the 1700 Cascadia earthquake, which is known with high confidence. The insignificance of including uncertainty in earthquake dates is demonstrated by the comparison of the Goldfinger et al. (2017) (3 earthquakes in the last 1000 years) and Nelson et al. (2021) (two earthquakes chronologies), where even including a different number of earthquakes does not significantly impact our results. The insensitivity to pre-1700 CSZ earthquakes in this methodology is shown in Fig. 4, where even in the 50 % coseismic landslide model, no discernible spike in landslide ages is seen around the circa 859 ybp earthquake. We also assume that any possible coeval ages between CSZ earthquakes and landslides implies a triggering relationship. The impact of this assumption implies our results are an upper limit to the true rates of coseismic landslide triggering, as landslide dams, or bedrock landslides, triggered by aseismic sources in the same year as a CSZ earthquake would be counted in our analysis as coseismic. However, slow moving landslides initiated by a past CSZ earthquake and forming a landslide dam, or stable deposit decades after the earthquake event are not included in this study due to our inability to assess the seismic origin of a landslide postdating known slides. While we assume this is a negligible effect in this dataset given the findings of Xu et al. (2021) that few landslides in the portion of the OCR we investigate are moving in the recent past, there may be landslides identified as aseismic in this study that had some degree of mobilization during some past CSZ earthquake.

We note the potential limits on coseismic landslide triggering modeled in this work are affected by the selection of landslide type and particular study region, preservation bias of young landslides, and modeling of past CSZ earthquake ages. Given the preponderance of landslides and relatively high rates of modern non-seismic triggering in the OCR, we expect a preservation bias toward younger deposits due to older landslides being eroded, covered by new landslides, or remobilized. Similarly, progressive decay of the ghost forests utilized by Struble et al. (2020, 2021) may introduce an additional preservation bias, where younger lakes with intact trees are more likely to be accurately dated. While preservation bias is accounted for in the modeling of synthetic landslide inventories, it reduces the likelihood of observing older, potentially coseismic, landslide deposits and may reduce our implied longer-term rates of Cascadia landslide triggering. However, estimates of landslide dam rates during the 1700 CSZ earthquake are relatively insensitive to the total population of landslide dams used in the initial phase of this work (e.g., using a total landslide dam population of 251 [25 additional landslide dams] shifts our upper bound estimate from 26 to 29 coseismic landslide dams), so the preservation of older landslide dammed lakes should not significantly affect our findings. Moreover, there is ample evidence for the preservation of very old (>40,000 ybp) bedrock landslides and dams in this landscape (Almond et al., 2007; Hammond et al., 2009; Roering et al., 2005). Our limited focus on landslide dams and deep-seated bedrock slides in the OCR omits additional candidate 1700 landslides that lack the dating precision and known total population of the OCR landslide dams (e.g., shallow slides) or that fall outside of our study region. However, landslides outside the OCR, like those along coastal bluffs (Schulz et al., 2012) and in the Olympic Mountains (Leithold et al., 2018), may reveal different coseismic sensitivity or along-strike variability during past CSZ earthquakes meriting further study. Additionally, shallow soil slides, often the most common type of landslide triggered by earthquakes (e.g., Keefer, 1984) were not considered in this study as they are unlikely to form

stable dams or meet the mapping criteria of LaHusen et al. (2020). These smaller, but potentially more numerous, coseismic landslides are likely unmappable at present due to natural and human changes to the landscape, but they may be preserved in lacustrine records of sedimentation (e.g., Richardson et al., 2018).

Using our upper bound estimate for coseismic landslide triggering, ~2400 large landslides (12 % of the ~20,000 mapped landslides) could occur just within the OCR during a single CSZ earthquake. This estimate of single-earthquake coseismic landslide triggering in the OCR is comparable to what was observed in well-documented landslide inventories from the 2011 Tohōku, Japan (Wartman et al., 2013), 2010 Maule, Chile (Serey et al., 2019), and 2007 Pisco, Peru (Lacroix et al., 2013) megathrust earthquakes, where hundreds to a few thousand landslides were mapped over the entire subaerial regions affected by strong shaking. Much higher estimates of landsliding from the 1964 M9.5 Great Alaska Earthquake where over 10,000 landslides may have been triggered by strong shaking, including highly destructive large deep-seated slides in Anchorage (Keefer and Wilson, 1989), may provide an upper limit on potential Cascadia-wide landslide triggering. While no landslides triggered by the 1700 CSZ earthquake have been conclusively identified in the OCR, our analysis of the available data do not require slow CSZ ruptures deficient in landslide-triggering, high-frequency energy as some have interpreted from offshore geomorphology (McAdoo et al., 2004) or otherwise weak shaking interpreted from paleoliquefaction (Obermeier, 1995).

5. Conclusions

To date, no precisely dated landslides attributable to earthquakes on the Cascadia Subduction Zone have been identified. However, a lack of recorded deep-seated landslides in the historical (~100 year) record has previously led to speculation that many or all large landslides in the Oregon Coast Range were triggered by past Cascadia megathrust earthquakes. To test this assumption, we used high-precision dendrochronology dates of landslide dammed lakes in the Oregon Coast Range and a large inventory of landslides dated via topographic roughness to place constraints on the percentage of landslides triggered by individual great Cascadia Subduction Zone earthquakes. Despite no current landslide dating to the last great Cascadia earthquake in 1700, the available record of 18 high-precision dates from a total of 226 landslide dams in the Oregon Coast Range (Struble et al., 2020, 2021) permit scenarios where up to 12 % of all landslide dams were triggered during the 1700 earthquake. Longer-term rates of coseismic landslide dam formation from landslide ages that overlap with the past two-three great Cascadia Subduction Zone earthquakes suggest that up to 22 % of all landslide dams may be triggered by earthquakes over multiple seismic cycles in the past ~1000 years. Simulations of synthetic landslide inventories, which constrain possible coseismic landslide triggering contributions to the observed temporal distribution of landslides in the central Oregon Coast Range (LaHusen et al., 2020), yield an estimated upper bound of ~12 % of all large bedrock landslides that may have been triggered by Cascadia Subduction Zone earthquakes across multiple earthquake cycles. Taken together, we estimate up to 15 % of all large (bedrock and dam forming) landslides currently found in the Oregon Coast Range may have been triggered by CSZ earthquakes in the past millennium, with smaller rates of landsliding expected during individual Cascadia Subduction Zone earthquakes. These findings greatly refine the conclusions of LaHusen et al. (2020), who suggested rainfall triggers the majority of deep-seated bedrock landslides in the OCR. While our findings suggest just a minority (0–15 %) of all landslide dams or large bedrock landslides in the Oregon Coast Range were directly triggered by recent Cascadia Subduction Zone earthquakes, the hazard and risk posed by the widespread triggering of up to thousands of deep-seated landslides, some of which would likely dam streams, remains significant. Future geochronology and modeling work to constrain coseismic landslide timing and triggering in Cascadia could reduce the uncertainty in the estimates we present here and help to identify portions of the landscape beyond the Oregon Coast Range most susceptible to the secondary hazards of a future Cascadia Subduction Zone earthquake.

Declaration of competing interest

The authors declare that they have no known competing financial interests or personal relationships that could have appeared to influence the work reported in this paper.

Data availability

Data will be made available on request.

Acknowledgements

This project was funded by the U.S. Geological Survey Earthquake Science Program. We thank two anonymous reviews and Jonathan Perkins for their constructive reviews that greatly improved this manuscript. Any use of trade, firm, or product names is for descriptive purposes only and does not imply endorsement by the U.S. Government.

References

Almond, P., Roering, J., Hales, T.C., 2007. Using soil residence time to delineate spatial and temporal patterns of transient landscape response. J. Geophys. Res. Earth Surf. 112 (F3) https://doi.org/10.1029/2006JF000568.

Anderson, K., 2009. In: The Ozette Prairies of Olympic National Park: Their Former Indigenous Uses and Management. Pacific West Region, National Park Service, pp. 1–158.

Atwater, B.F., Hemphill-Haley, E., 1997. Recurrence Intervals for Great Earthquakes of the Past 3,500 Years at North-eastern Willapa Bay, Washington. (US Geological Survey Professional Paper 1576). https://doi.org/10.3133/pp1576.

Atwater, B.F., Musumi-Rokkaku, S., Satake, K., Tsuji, Y., Ueda, K., Yamaguchi, D.K., 2005. The Orphan Tsunami of 1700. University of Washington Press, Seattle, WA.

Bommer, J.J., Rodríguez, C.E., 2002. Earthquake-induced landslides in Central America. Eng. Geol. 63 (3-4), 189–220. https://doi.org/10.1016/S0013-7952(01)00081-3.

Booth, A.M., LaHusen, S.R., Duvall, A.R., Montgomery, D.R., 2017. Holocene history of deep-seated landsliding in the North Fork Stillaguamish River valley from surface roughness analysis, radiocarbon dating, and numerical landscape evolution modeling. J. Geophys. Res. Earth Surf. 122, 456–472. https://doi.org/10.1002/2016jf003934.

Bush, C., 2020. Landslide ages and implications for a marine terrace at Rialto Beach, WA. Retrieved from. University of Washington, Seattle, USA. https://digital.lib.washington.edu/.

Fan, X., Scaringi, G., Korup, O., West, A.J., van Westen, C.J., Tanyaş, H., Huang, R., 2019. Earthquake-induced chains of geologic hazards: patterns, mechanisms, and impacts. Rev. Geophys. 57 (2), 421–503. https://doi.org/10.1029/2018RG000626.

Franczyk, J.J., Burns, W.J., Calhoun, N.C., 2019. Statewide landslide information database for Oregon release-4.0, SLIDO 4.0. (Oregon Department of Geology and Mineral Industries, Digital Data Series). Available at. https://www.oregongeology.org/slido/.

Goldfinger, C., Nelson, C.H., Morey, A.E., Johnson, J.E., Patton, J.R., Vallier, T., 2012. Turbidite Event History—Methods and Implications for Holocene Paleoseismicity of the Cascadia Subduction Zone. (US Geological Survey Professional Paper 1661-F). https://doi.org/10.3133/pp1661F.

Goldfinger, C., Galer, S., Beeson, J., Hamilton, T., Black, B., Romsos, C., Morey, A., 2017. The importance of site selection, sediment supply, and hydrodynamics: a case study of submarine paleoseismology on the northern Cascadia margin, Washington USA. Mar. Geol. 384, 4–46. https://doi.org/10.1016/j.margeo.2016.06.008.

Hammond, C.M., Meier, D., Beckstrand, D.L., 2009. Paleo-landslides in the Tyee Formation and highway construction, central Oregon Coast Range. In: Geological Society of America Field Guide, 15, pp. 481–494. https://doi.org/10.1130/2009.fld015(23).

Jibson, R.W., Tanyaş, H., 2020. The influence of frequency and duration of seismic ground motion on the size of triggered landslides—a regional view. Eng. Geol. 273, 105671 https://doi.org/10.1016/j.enggeo.2020.105671.

Karlin, R.E., Holmes, M., Abella, S.E.B., Sylwester, R., 2004. Holocene landslides and a 3500-year record of Pacific Northwest earthquakes from sediments in Lake Washington. Geol. Soc. Am. Bull. 116 (1–2), 94–108. https://doi.org/10.1130/B25158.1.

Keefer, D.K., 1984. Landslides caused by earthquakes. Geol. Soc. Am. Bull. 95 (4), 406–421.

Keefer, D.K., Wilson, R.C., 1989. Predicting Earthquake-Induced Landslides with Emphsasis on Arid and Semi-Arid Environments. Inland Geol. Soc. 2, 118–149.

Kelsey, H.M., Witter, R.C., Hemphill-Haley, E., 2002. Plate-boundary earthquakes and tsunamis of the past 5500 yr, Sixes River estuary, southern Oregon. GSA Bull. 114 (3), 298–314. https://doi.org/10.1130/0016-7606(2002)114<0298:PBEATO>2.0.CO;2.

Lacroix, P., Zavala, B., Berthier, E., Audin, L., 2013. Supervised method of landslide inventory using panchromatic SPOT5 Images and Application to the Earthquake-Triggered Landslides of Pisco (Peru, 2007, Mw8.0). Remote Sens. 5, 2590–2616. https://doi.org/10.3390/rs5062590.

LaHusen, S.R., Duvall, A.R., Booth, A.M., Montgomery, D.R., 2016. Surface roughness dating of long-runout landslides near Oso, Washington (USA), reveals persistent postglacial hillslope instability. Geology 44, 111–114. https://doi.org/10.1130/g37267.1.

LaHusen, S.R., Duvall, A.R., Booth, A.M., Grant, A., Mishkin, B.A., Montgomery, D.R., 2020. Rainfall triggers more deep-seated land- slides than Cascadia earthquakes in the Oregon Coast Range, USA. Sci. Adv. 6, eaba6790 https://doi.org/10.1126/sciadv.aba6790.

Leithold, E.L., Wegmann, K.W., Bohnenstiehl, D.R., Smith, S.G., Noren, A., O'Grady, R., 2018. Slope failures within and upstream of Lake Quinault, Washington, as uneven responses to Holocene earthquakes along the Cascadia subduction zone. Quat. Res. 89 (1), 178–200. https://doi.org/10.1017/qua.2017.96.

Ludwin, R.S., Dennis, R., Carver, D., McMillan, A.D., Losey, R., Clague, J., Jonientz-Trisler, C., Bowechop, J., Wray, J., James, K., 2005. Dating the 1700 Cascadia Earthquake: Great Coastal Earthquakes in Native Stories. Seismol. Res. Let. 76 (2), 140–148.

Marc, O., Hovius, N., Meunier, P., Gorum, T., Uchida, T., 2016. A seismologically consistent expression for the total area and volume of earthquake-triggered landsliding. J. Geophys. Res. Earth Surf. 121 (4), 640–663. https://doi.org/10.1002/2015JF003732.

McAdoo, B.G., Capone, M.K., Minder, J., 2004. Seafloor geomorphology of convergent margins: Implications for Cascadia seismic hazard. Tectonics 23. https://doi.org/10.1029/2003TC001570.

McPhillips, D., Scharer, K.M., 2021. Survey of fragile geologic features and their quasi-static earthquake ground-motion constraints, Southern Oregon. Bull. Seismol. Soc. Am. https://doi.org/10.1785/0120200378.

Meunier, P., Hovius, N., Haines, A.J., 2007. Regional patterns of earthquake-triggered landslides and their relation to ground motion. Geophys. Res. Lett. 34 (20) https://doi.org/10.1029/2007GL031337.

Montgomery, D.R., 2001. Slope distributions, threshold hillslopes, and steady-state topography. Am. J. Sci. 301, 432–454. https://doi.org/10.2475/ajs.301.4-5.432.

Nelson, A.R., Atwater, B.F., Bobrowsky, P.T., Bradley, L.-A., Clague, J.J., Stuiver, M., 1995. Radiocarbon evidence for extensive plate-boundary rupture about 300 years ago at the Cascadia subduction zone. Nature 378 (6555), 371–374. https://doi.org/10.1038/378371a0.

Nelson, A.R., Kelsey, H.M., Witter, R.C., 2006. Great earthquakes of variable magnitude at the Cascadia subduction zone. Quat. Res. 65 (3), 354–365. https://doi.org/10.1016/j.yqres.2006.02.009.

Nelson, A.R., DuRoss, C.B., Witter, R.C., Kelsey, H.M., Engelhart, S.E., Mahan, S.A., Padgett, J.S., 2021. A maximum rupture model for the central and southern Cascadia subduction zone—reassessing ages for coastal evidence of megathrust earthquakes and tsunamis. Quat. Sci. Rev. 261, 106922 https://doi.org/10.1016/j.quascirev.2021.106922.

Obermeier, S.F., 1995. Preliminary Estimates of the Strength of Prehistoric Shaking in the Columbia River Valley and the Southern Half of Coastal Washington, With Emphasis for a Cascadia Subduction Zone Earthquake About 300 Years pago. (US Geological Survey Open File Report 94–589). https://doi.org/10.3133/ofr94589.

Oregon Lidar Consortium and Oregon Department of Geology and Mineral Industries, 2022. Bare Earth lidar digital elevation model. Retrieved from. https://www.oregongeology.org/lidar/.

Penserini, B.D., Roering, J.J., Streig, A., 2017. A morphologic proxy for debris flow erosion with application to the earthquake deformation cycle, Cascadia Subduction Zone, USA. Geomorphology 282, 150–161. https://doi.org/10.1016/j.geomorph.2017.01.018.

Petley, D., 2012. Global patterns of loss of life from landslides. Geology 40 (10), 927–930. https://doi.org/10.1130/G33217.1.

Pringle, P.T., 2014. Buried and submerged forests of Washington and Oregon: time capsules of environmental and geologic history. Western Forester 59 (14–15), 22.

Rasanen, R.A., Marafi, N.A., Maurer, B.W., 2021. Compilation and forecasting of paleoliquefaction evidence for the strength of ground motions in the US Pacific Northwest. Eng. Geol. 292, 106253 https://doi.org/10.1016/j.enggeo.2021.106253.

Richardson, K.N.D., Hatten, J.A., Wheatcroft, R.A., 2018. 1500 years of lake sedimentation due to fire, earthquakes, floods and land clearance in the Oregon Coast Range: geomorphic sensitivity to floods during timber harvest period. Earth Surf. Process. Landforms 43, 1496–1517. https://doi.org/10.1002/esp.4335.

Roering, J.J., Kirchner, J.W., Dietrich, W.E., 2005. Characterizing structural and lithologic controls on deep-seated landsliding: Im- plications for topographic relief and landscape evolution in the Oregon Coast Range, USA. Geol. Soc. Am. Bull. 117, 654. https://doi.org/10.1130/b25567.1.

Satake, K., Wang, K., Atwater, B.F., 2003. Fault slip and seismic moment of the 1700 Cascadia earthquake inferred from japanese tsunami descriptions. J. Geophys. Res. Solid Earth 108 (B11), 2535. https://doi.org/10.1029/2003JB002521.

Schmidt, K.M., Roering, J.J., Stock, J.D., Dietrich, W.E., Montgomery, D.R., Schaub, T., 2001. The variability of root cohesion as an in- fluence on shallow landslide susceptibility in the Oregon Coast Range. Can. Geotech. J. 38, 31. https://doi.org/10.1139/t01-031.

Schulz, W.H., Galloway, S.L., Higgins, J.D., 2012. Evidence for earthquake triggering of large landslides in coastal Oregon, USA. Geomorphology 141–142, 88–98. https://doi.org/10.1016/j.geomorph.2011.12.026.

Serey, A., Piñero-Feliciangeli, L., Sepúlveda, S.A., Poblete, F., Petley, D.N., Murphy, W., 2019. Landslides induced by the 2010 Chile megathrust earthquake: a comprehensive inventory and correlations with geological and seismic factors. Landslides 16, 1153–1165. https://doi.org/10.1007/s10346-019-01150-6.

Šilhán, K., 2020. Dendrogeomorphology of landslides: Principles, results and perspectives. Landslides. https://doi.org/10.1007/s10346-020-01397-4.

Stock, J., Dietrich, W.E., 2003. Valley incision by debris flows: evidence of a topographic signature. Water Resour. Res. 39 https://doi.org/10.1029/2001wr001057.

Struble, W.T., Roering, J.J., Black, B.A., Burns, W.J., Calhoun, N., Wetherell, L., 2020. Dendrochronological dating of landslides in western Oregon: searching for signals of the Cascadia A.D. 1700 earthquake. Geol. Soc. Am. Bull. 130, 17. https://doi.org/10.1130/B35269.1.

Struble, W.T., Roering, J.J., Burns, W.J., Calhoun, N.C., Wetherell, L.R., Black, B.A., 2021. The preservation of climate-driven landslide dams in Western Oregon. J. Geophys. Res. Earth Surf. 126 (4), e2020JF005908 https://doi.org/10.1029/2020JF005908.

Tanyaş, H., Van Westen, C.J., Allstadt, K.E., Anna Nowicki Jessee, M., Görüm, T., Jibson, R.W., Hovius, N., 2017. Presentation and analysis of a worldwide database of earthquake-induced landslide inventories. J. Geophys. Res. Earth Surf. 122 (10), 1991–2015. https://doi.org/10.1002/2017JF004236.

Valagussa, A., Marc, O., Frattini, P., Crosta, G.B., 2019. Seismic and geological controls on earthquake-induced landslide size. Earth Planet. Sci. Lett. 506, 268–281. https://doi.org/10.1016/j.epsl.2018.11.005.

Walton, M.A., Staisch, L.M., Dura, T., Pearl, J.K., Sherrod, B., Gomberg, J., Wirth, E., 2021. Toward an integrative geological and geophysical view of Cascadia subduction zone earthquakes. Annu. Rev. Earth Planet. Sci. 49, 367–398. https://doi.org/10.1146/annurev-earth-071620-065605.

Wartman, J., Dunham, L., Tiwari, B., Pradel, D., 2013. Landslides in Eastern Honshu Induced by the 2011 Off the Pacific Coast of Tohoku Earthquake. Bull. Seismol. Soc. Am. 103 (2B), 1503–1521. https://doi.org/10.1785/0120120128.

Wirth, E.A., Grant, A., Marafi, N.A., Frankel, A.D., 2021. Ensemble ShakeMaps for magnitude 9 earthquakes on the Cascadia subduction zone. Seismol. Soc. Am. 92 (1), 199–211. https://doi.org/10.1785/0220200240.

Witter, R.C., Kelsey, H.M., Hemphill-Haley, E., 2003. Great Cascadia earthquakes and tsunamis of the past 6700 years, Coquille River estuary, southern coastal Oregon. GSA Bull. 115 (10), 1289–1306. https://doi.org/10.1130/B25189.1.

Xu, Y., Schulz, W.H., Lu, Z., Kim, J., Baxstrom, K., 2021. Geologic controls of slow-moving landslides near the US West Coast. Landslides 18 (10), 3353–3365. https://doi.org/10.1007/s10346-021-01732-3.